Zn(II) and Ni(II) complexes with poly-histidyl peptides derived from a snake venom

Article *in* Inorganica Chimica Acta · June 2017

DOI: 10.1016/j.ica.2017.05.070

Inorganica Chimica Acta xxx (2017) xxx–xxx

Contents lists available at ScienceDirect

Inorganica Chimica Acta

journal homepage: www.elsevier.com/locate/ica

Research Paper

Zn(II) and Ni(II) complexes with poly-histidyl peptides derived from a snake venom

Maurizio Remelli [a,*], Davide Brasili [a], Remo Guerrini [a], Fabio Pontecchiani [a], Slawomir Potocki [b], Magdalena Rowinska-Zyrek [b], Joanna Watly [b], Henryk Kozlowski [c]

[a] Department of Chemical and Pharmaceutical Sciences, University of Ferrara, via L. Borsari 46, 44121 Ferrara, Italy
[b] Faculty of Chemistry, University of Wroclaw, Wroclaw, Poland
[c] High Professional Medical School in Opole, Opole, Poland

ARTICLE INFO

Article history:
Received 29 April 2017
Received in revised form 23 May 2017
Accepted 30 May 2017
Available online xxxx

Keywords:
Zinc ion
Nickel ion
Snake venom
Poly-His peptides
Complex-formation equilibria

ABSTRACT

The snake venoms are complex mixtures containing many bioactive peptides and proteins; some of them are aimed to protect the snake glands, where the venom is stored, until the latter is inoculated in the victim. In the venom of some vipers of the genus *Atheris*, a set of peptides containing poly-His and poly-Gly segments was recently found. Poly-His peptides are not rare in Nature. Although their exact biological function is most often unknown, one thing is certain: they have good binding properties towards the transition metal ions. As a matter of fact, the imidazole side chain of histidine is one of the groups most frequently involved in metal complexation in the active sites of metallo-enzymes. This is also true for snake-venom metallo-proteases, which contain Zn(II) and Ca(II) ions.

In the present paper, the complex-formation ability of the poly-His-poly-Gly peptide found in the venom of *Atheris squamigera* ($EDDH_9GVG_{10}$-NH_2) towards the Zn(II) and Ni(II) ions was investigated by means of thermodynamic and spectroscopic techniques. Two model peptides, derived from the poly-His portion of this peptide but where His residues were alternated with alanines (Ac-EDDAHAHAHAHAG-NH_2, and Ac-EDDHAHAHAHAHG-NH_2) were also studied, for the sake of comparison. The high affinity of these peptides for the metal ions under investigation was confirmed. In addition, it was demonstrated that the number of His residues in the peptide and their relative position play a main role in the complex-formation ability of the ligand. The very high affinity of $EDDH_9GVG_{10}$-NH_2 for Zn(II) can be the key for its role in the inactivation of the venom in the snake glands.

1. Introduction

The snake venoms are complex mixtures containing hundreds of toxins [1] from which valuable active ingredients for several drugs have been derived, such as those used for the treatment of cardiovascular diseases, for the relief of pain or for the skin care [2]. The venoms of different snake families have been recently successfully tested for their cytotoxic effect against breast and skin cancer cells [3]. The main enzymes in most snake venoms are metalloproteinases (SVMPs) [4], which are responsible for their haemorrhagic activity. The SVMPs are phylogenetically related to the family of adamalysin (or ADAM) and usually contain calcium and/or zinc ions [1]. The zinc-binding domain is highly conserved throughout the ADAM family and contains three histidine residues separated by three and five amino acids, respectively (-HEXXHXXGXXH-) [5]; the histidines are bound to the zinc ion together with a water molecule in a tetrahedral structure [1].

Since the SVMPs contained in the snake venom can induce severe local and systemic bleeding in the victim, why the venom stored in the snake glands does not damage the snake itself? The advanced hypotheses to answer this question derive from the fact that high concentrations of citrate and peptides with metal-ligand capabilities have been found in venoms and that the pH in the snake gland is about 5. The activity of SVMPs in the snake glands would therefore be inhibited by three synergistic mechanisms: (i) chelation of calcium by citrate anion; (ii) acidic pH and (iii) enzyme inhibition by specific peptides [6]. Once the venom is injected into the victim's blood, its dilution and the physiological pH cancel the inhibitory mechanisms.

It has been shown that the snake venoms disturb the homeostasis of some metal ions of the victim: a significant increase of copper

* Corresponding author.
E-mail address: maurizio.remelli@unife.it (M. Remelli).

http://dx.doi.org/10.1016/j.ica.2017.05.070
0020-1693/

levels in serum was observed [7] and it was suggested to use copper/zinc ratio in the serum as a marker of effects of poisoning [8]. On the other hand, it was instead demonstrated that copper can act as an inhibitor against serine proteases and metalloproteinases [9,10], according to a mechanism not yet fully explained.

An investigation on the venoms from snakes of the genus *Atheris* showed that they contain a set of poly-His/poly-Gly peptides (pHpG) [11]. In particular, the peptide $EDDH_9GVG_{10}$, characterized by the presence of nine consecutive His residues, has the ability of neutralizing the haemorrhagic activity of the *Echisocellatus* venom [12].

Besides the venom of snakes, His-rich proteins (HRP) have been found in many living organisms [12–17]. They can play crucial roles in many aspects of the life [18] included the transport of metal ions into/through the organism [19], as it happens for the two zinc-binding proteins AdcA and AdcAII which are critical for zinc feeding in Streptococcus pneumoniae [20]. Several HRPs contain at least one His-tag region [13,17,21,22] which is very effective to bind metal ions and can be exploited for the purification of such proteins through Immobilized Metal Ion Affinity Chromatography (IMAC). The His-tag (usually His_6-tag) can be also artificially added to the sequence of the protein [23,24]. In fact, the imidazole nitrogens of histidine side chains are able to form strong coordination bonds with metal cations such as Ni(II), Cu(II), Co(II) or Zn(II), immobilized into the chromatographic stationary phase [25–27].

Our research group has recently studied the binding properties of the protected peptides $EDDH_9GVG_{10}$-NH_2 (L3) and Ac-$EDDH_9G$-NH_2 [28,29]. The presence of nine histidine residues in a row (His_9-tag) makes these fragments very efficient metal chelators, also in comparison to other His-rich peptides. Most interestingly, it was demonstrated the His_9-tag acts as a "polymorphic binding site", since different sets of imidazoles can bind the metal ion in different ways thus allowing it to "move along" the poly-His sequence. In addition, the metal binding induces the formation of a regular α-helical structure. A similar behaviour was also found for the Cu(II) complexes with the His_6-tag [30,31].

In order to shed more light on the coordination modes of the (His_9-tag), the above study was recently extended to two analogues of Ac-$EDDH_9G$-NH_2 in which some His residues were mutated to alanines [32]: the number of histidines is reduced and they are no longer consecutive. The first peptide contains four His residues alternating with five Ala residues (Ac-EDDAHAHAHAHAG-NH_2, L1) while the second one consists of five His residues alternating with four alanines (Ac-EDDHAHAHAHAHG-NH_2, L2). The latter study has demonstrated that the presence of 4 or 5 histidines makes both peptides L1 and L2 excellent ligands for the Cu(II) ion. However, it was confirmed, in agreement with the previous literature [14,33–35], that the total number of histidines in the ligand rules the stability of the formed Cu(II) complexes, also if an equal number of imidazole groups is coordinated to copper. As a matter of fact, a lower number of available histidines reduces the number of possible binding combinations.

It is well known that imidazole side chain of His is a good binding site not only for Cu(II) but also for other biologically relevant metal ions, as Zn(II) and Ni(II). While the latter shares with Cu(II) the capability of displacing the amidic protons of the peptidic backbone [36,37], zinc does not have this capacity but it is able to form stable poly-His complexes [38,39]. In order to complete the survey on the behaviour of pHpG peptides derived from *Atheris Squamigera*, in the present paper a thermodynamic and spectroscopic study on the formation of Ni(II) and Zn(II) complexes with the three peptides Ac-EDDAHAHAHAHAG-NH_2 (L1), Ac-EDDHAHAHAHAHG-NH_2 (L2) and $EDDH_9GVG_{10}$-NH_2 (L3) is described; the results are compared with those previously described in the literature for these ligands with Cu(II) and for other poly-His peptides with Ni(II) and Zn(II).

2. Experimental

2.1. Materials

The synthesis of peptides Ac-EDDAHAHAHAHAG-NH_2 (L1) and Ac-EDDHAHAHAHAHG-NH_2 (L2) is describes elsewhere [32]. The C-protected peptide $EDDH_9GVG_{10}$-Am (L3) was purchased from Selleck Chemicals (Huston, TX) (certified purity: 99.35%) and used as received. The purity of the three ligands was potentiometrically checked.

$NiCl_2$ and $ZnCl_2$ were extra pure products (Sigma-Aldrich); their stock solutions were standardized by EDTA titration and periodically checked *via* ICP-MS. The carbonate-free stock solution of KOH (Sigma-Aldrich) was potentiometrically standardized with the primary standard potassium hydrogen phthalate. The HCl stock solution was prepared by diluting concentrated HCl (Sigma-Aldrich) and standardized with standard KOH. All sample solutions were prepared using freshly doubly-distilled water. The ionic strength was adjusted to 0.1 mol dm^{-3} by adding suitable amounts of KCl (Sigma-Aldrich). Grade A glassware was employed throughout.

2.2. Potentiometric measurements

Protonation and complex-formation constants were calculated from potentiometric titration curves recorded in the pH range 2.5–10.5; the sample solution volume was 1.5 cm^3. The pH-metric titrations were performed with a MOLSPIN pH-meter system equipped with a Russell CMAW711 semi-micro, glass, combination pH electrode, daily calibrated in proton concentration using HCl [40]. KOH was added into the titration cell with a 0.500 cm^3 micrometer syringe, previously calibrated. The delay time between two additions of titrant was suitable to guarantee the attainment of equilibrium; the kinetics of complex-formation was fast with zinc but rather slow with nickel, especially in the alkaline pH range. The ligand concentration was always about $5 \cdot 10^{-4}$ mol dm^{-3} and the metal/ligand ratio was 1:1.2. The temperature the sample solution of was kept at 298.2 ± 0.1 K by means of a circulation thermostat. High purity grade argon was gently blown over the test solution in order to maintain an inert atmosphere. Constant-speed magnetic stirring was applied throughout.

The standard potential and the slope of the electrode couple were computed from the calibration titrations by means of Glee [41] or SUPERQUAD [42] programs. The exact concentration of the ligand in each sample solution was determined with the Gran method [43]. The HYPERQUAD program [44] was employed for the calculation of the overall (β_{pqr}) stability constant, referred to the following equilibrium:

$$pM + qL + rH \rightleftarrows M_pL_qH_r \quad (1)$$

(charges omitted; p is 0 in the case of ligand protonation; r can be negative). Reported K_a values are instead the acid dissociation constants of the corresponding species. The computed standard deviations (referring to random errors only) are shown in parentheses as uncertainties on the last significant figure. The distribution diagrams were computed with the HYSS program [45]. Metal hydrolysis constants were taken from the literature [46]. A pK_w value of 13.77 was used and checked through separate experiments.

The stability constant values of complexes with different stoichiometries and/or protonation degrees cannot be directly compared. The overall metal binding ability can instead be evaluated in a wide pH range by computing and plotting the competition diagrams, starting from the binary speciation models. A solution containing the metal and the two (or more) ligands (or *vice versa*) is simulated, admitting that all the components compete with each

other to form the respective binary complexes, without that any mixed species is formed. This is a reasonable approximation in the case of peptides, which most often form only 1:1 complexes in which the peptide completely wraps the metal ion.

2.3. Spectroscopic measurements

The absorption spectra were recorded on a Varian Cary 300 Bio spectrophotometer, in the range 200–800 nm, using a quartz cuvette with an optical path of 1 cm. Circular dichroism (CD) spectra were recorded on Jasco J 715 spectropolarimeter in the 230–800 nm range, using a quartz cuvette with an optical path of either 1.0 cm or 0.1 cm for the visible and UV wavelengths, respectively. The concentration of solutions used for spectroscopic studies were similar to those employed in potentiometry.

2.4. Mass spectrometric measurements

High-resolution mass spectra were obtained on a BrukerQ-FTMS spectrometer (BrukerDaltonik, Bremen, Germany), equipped with an Apollo II electrospray ionization source with an ion funnel. The mass spectrometer was operated in both the positive and the negative ion mode. The instrumental parameters were as follows: scan range m/z 400–1600, dry gas nitrogen, temperature 170 °C, ion energy 5 eV. Capillary voltage was optimized to the highest S/N ratio (4500 V). Small changes of voltage (±500 V) did not significantly affect the optimized spectra. The samples (metal/ligand 1:1.2 or 2:1, $[\text{ligand}]_{tot} = 5 \cdot 10^{-4}$ mol dm^{-3}) were prepared in 1:1 MeOH-H_2O mixture. The sample was infused at a flow rate of 3 μL/min. The instrument was externally calibrated with the Tunemix™ mixture (BrukerDaltonik, Germany) in quadratic regression mode. Data were processed by using the Bruker Compass DataAnalysis 4.0 program. The mass accuracy for the calibration was better than 5 ppm, enabling together with the true isotopic pattern (using SigmaFit) an unambiguous confirmation of the elemental composition of the obtained complex.

3. Results and discussion

3.1. Protonation equilibria

Protonation constants for the ligands under investigation have been previously measured and are discussed elsewhere [28,32]. For the sake of clarity they are reported in Table 1, while the corresponding distribution diagrams are reported as Supplementary information (Fig. S1).

3.2. Ni(II) complexes

The three peptides are able to form stable 1:1 complexes with the Ni(II) ions; no poly-nuclear or bis-complexes have been detected neither by potentiometry nor by mass spectrometry. Formation constant values are shown in Table 2 and the corresponding distribution diagrams are plotted in Fig. 1; ESI-MS results are instead reported as Supplementary Information (Figs. S2 and S3).

The two short mutants L1 and L2 form five protonated mononuclear Ni(II) complexes with the same stoichiometry already reported for Cu(II) [32], even though the corresponding $\log\beta$ values are lower of about 3 orders of magnitude. The presence in solution of Ni(II) mono-complexes is confirmed by ESI-MS (see Supplementary Information). The distribution diagrams (Fig. 1) show that the complex-formation starts at pH 4.0–4.5; the first detected complex is $[NiLH_2]^+$ for L1 and $[NiLH_3]^{2+}$ for L2. The stoichiometry of these species suggests that both the three acidic side chains of Asp and Glu and two His residues are deprotonated: since the lowest pK_a value for imidazole side chains for both L1 and L2 is 5.61 (see Table 1), these two His residues can be deprotonated at pH 4.5 only if their protons have been displaced by the metal ion. Therefore, $[NiLH_2]^+$ for L1 and $[NiLH_3]^{2+}$ for L2 should be ($2N_{Im}$) complexes, with the remaining coordination positions around the metal ion occupied by oxygen atoms. The weak d-d bands in the Vis absorption spectra measured at acidic pH (Fig. 2) suggests that these complexes have a hexacoordinate, high-spin, octahedral geometry. The oxygen donors can either derive from water molecules or carboxylate groups belonging to the Asp or Glu residues.

The most abundant species at neutral pH is $[NiL]^-$ for L1 and [NiLH] for L2: Vis spectra do not show relevant changes when pH is increased from 5 to 7, thus suggesting that the octahedral geometry is maintained. However, it is possible that three or even four imidazole nitrogens are now bound to nickel. The stoichiometry of [NiLH] imposes that the fifth His of L2 is protonated; the release of this proton, giving rise to the complex $[NiL]^-$, is characterized by a pK_a value of 7.89 (Table 2), rather close to that of the most basic His residue of free L2 (7.72, Table 1), suggesting that this residue does not take part in complexation.

CD spectra (Fig. 3) reveal [47] that the interaction of the Ni(II) ion with amide nitrogens starts at pH close to 9, therefore with the formation of the species $[NiLH_{-1}]^{2-}$, both for L1 and L2. At the same time, the wavelength of maximum absorption blue-shifts to 440 nm, suggesting a change in the complex geometry from octahedral to square planar geometry for this species and also for those formed at higher pH. It is worth of note that the complex $[NiLH_{-2}]^{3-}$ is not detected in both the systems. It can be inferred that nickel, once bound to the first amide nitrogen, exploits the alkaline pH value and the proximity of the backbone chain to cooperatively bind two additional amide nitrogens, thus forming the species $[NiLH_{-3}]^{4-}$.

Due to the similar structure of the two peptides, it is possible to directly compare $\log\beta$ values of the corresponding $[NiL]^-$ species: rather unexpectedly, the complex formed by L1 is more stable than that of L2, with a difference in the $\log\beta$ values of 1.1 orders of magnitude. This behaviour is opposite of that found with Cu(II) [32]. This result supports the hypothesis of the absence of an axial interaction of the fifth imidazole of L2 with the metal ion, as instead previously suggested for Cu(II) [32]. The competition plot reported in Fig. 4 describes the situation in the whole pH range. There is not a big difference in the metal affinity of the two ligands until pH 6.5, where the ($4\ N_{Im}$) species ($[NiL]^-$ for L1 and [NiLH] for L2) starts to form in both cases. Considering that the coordination environment is the same, the higher stability of the former one can be simply due to the difference in the ligand charge. On the other hand, is not trivial to explain the difference in stability of the complexes formed at alkaline pH, where the charge is the same for the two ligands. Here, the complex geometry changes to square planar and up to three amide nitrogens bind the Ni(II) ion in substitution of imidazole rings. This point would require further investigation, e.g. by means of NMR spectroscopy and theoretical computations.

Finally, in Fig. S4 (Supplementary Information) the coordination ability of L1 and L2 towards the Ni(II) ion is compared to that of the peptide Ac-THHHHAHGG-NH_2 [14] which has five His residues. The latter results a ligand for Ni(II) stronger than both L1 and L2, especially in the alkaline pH range, where all the nickel complexes are square planar and the amide nitrogens take part in complexation. The closer proximity of the His residues in Ac-THHHHAHGG-NH_2 increases the complex stability, possibly due to stacking interaction between the neighbouring imidazole rings.

The formation of nickel complexes with L3 starts around pH 4. Unfortunately, the Ni(II)/L3 solutions became turbid in the pH range 6–9; they returned clear at strongly alkaline pH. For this reason, the processing of potentiometric data was considered reliable only at acid pH (3–6); the speciation model of Table 2 and the

Table 1
Protonation constants for the peptides, at T = 298 K and I = 0.1 mol dm^{-3} (KCl). Standard deviations on the last figure in parentheses. Data for L1 and L2 are from Ref. [32]; data for L3 are from Ref. [28].

Ligand	Species	Log β	pK_a	Residue
L1	LH^{2-}	7.89 (6)	7.89	His
	LH_2^-	14.47 (6)	6.58	His
	LH_3	20.98 (7)	6.51	His
	LH_4^+	26.59 (7)	5.61	His
	LH_5^{2+}	30.91 (9)	4.32	Glu
	LH_6^{3+}	34.49 (9)	3.58	Asp
	LH_7^{4+}	37.2 (1)	2.7	Asp
L2	LH^{2-}	7.72 (3)	7.72	His
	LH_2^-	14.54 (3)	6.82	His
	LH_3	21.17 (4)	6.63	His
	LH_4^+	27.14 (4)	5.97	His
	LH_5^{2+}	32.75 (5)	5.61	His
	LH_6^{3+}	37.01 (6)	4.26	Glu
	LH_7^{4+}	40.70 (7)	3.69	Asp
	LH_8^{5+}	43.23 (8)	2.53	Asp
L3	LH^{2-}	8.61 (3)	8.61	Amine
	LH_2^-	15.85 (4)	7.24	His
	LH_3	22.96 (4)	7.11	His
	LH_4^+	29.31 (6)	6.35	His
	LH_5^{2+}	35.57 (5)	6.26	His
	LH_6^{3+}	41.34 (5)	5.77	His
	LH_7^{4+}	46.72 (4)	5.38	His
	LH_8^{5+}	51.83 (3)	5.11	His
	LH_9^{6+}	55.99 (3)	4.16	His
	LH_{10}^{7+}	59.04 (3)	3.05	His
	LH_{11}^{8+}	61.06 (4)	2.02	Glu

Table 2
Cumulative complex-formation (β) and deprotonation (K_a) constants for binary Ni(II) complexes of the peptides L1, L2 and L3, at T = 298 K and I = 0.1 mol dm^{-3} (KCl). Standard deviations on the last figure in parentheses.

Ligand	Species	Log β	pK_a
L1	$[NiLH_2]^+$	18.94 (3)	5.80
	[NiLH]	13.14 (2)	6.29
	$[NiL]^-$	6.85 (2)	8.86
	$[NiLH_{-1}]^{2-}$	−2.01 (3)	–
	$[NiLH_{-3}]^{4-}$	−20.85 (3)	–
L2	$[NiLH_3]^{2+}$	25.33 (4)	–
	[NiLH]	13.66 (2)	7.89
	$[NiL]^-$	5.77 (6)	9.20
	$[NiLH_{-1}]^{2-}$	−3.43 (6)	–
	$[NiLH_{-3}]^{4-}$	−22.70 (7)	–
L3	$[NiLH_6]^{5+}$	45.31 (4)	5.19
	$[NiLH_5]^{4+}$	40.12 (2)	–
	$[NiLH_3]^{2+}$	29.25 (4)	6.14
	$[NiLH_2]^+$	23.11 (6)	6.0
	[NiLH]	17.1 (2)	6.4
	$[NiL]^-$	10.7 (1)	–

corresponding distribution diagram (Fig. 1c) are referred to this pH range. Fig. 1c shows that the first complex revealed by the potentiometric measurements is the species $[NiLH_6]^{5+}$ which reaches its maximum at pH 5. Considering the pK_a values of the free ligand (Table 1) the six protonated sites should correspond to the terminal amine and five His residues. Therefore, four imidazole side chains should be deprotonated and available to chelate the Ni(II) ion with the possible cooperation of three carboxylate groups. The involvement in complex-formation of the deprotonated terminal amine could also be inferred, but it does not look likely. It is not possible to know from the available data how many and which donor groups are bound to the metal, while it is possible to hypothesize that a number of different species, probably octahedral, with the same stoichiometry but different donor-atom sets are present in solution at the same time and in equilibrium each other.

When pH is increased, up to five protons are released by the complex, leading to the formation of the species [NiHL], starting from pH 5.5. Since turbidity is observed at pH close to 6, it can be suggested the precipitation of this neutral complex. From the appearance of a CD absorption band around pH 7 (Fig. S6, Supplementary Information) we can postulate the formation of a coordination bond Ni-N_{amide}. This absorption band becomes more and more intense as the pH value increases, thus suggesting the coordination of more amide nitrogens to the metal ion.

The presence of nine consecutive His residues in L3 allows it to complex the Ni(II) ion more strongly than the short peptides L1 and L2. This is evident from the competition diagram reported in Fig. S7 (Supplementary Information); unfortunately, the comparison is possible only in the acidic pH range due to the solubility problems of the Ni(II)/L3 complexes.

3.3. Zn(II) complexes

Under the equimolar metal/ligand experimental conditions employed for the potentiometric experiments, the three peptides form mono-nuclear Zn(II) complexes, as confirmed by ESI-MS spectra shown as Supplementary Information; their formation constant values are reported in Table 3 and the corresponding distribution diagrams are shown in Fig. 5.

The formation of zinc complexes with the two ligands L1 and L2 starts around pH 4.5; no precipitation has been observed over the explored pH range (3–11). The speciation models suggest the formation of five differently protonated mononuclear complexes with L1 and six with L2; this difference is simply due to the different number of His residues in the two peptides. Considering that the zinc ion is normally unable to displace amide protons, the complexation pattern is easy to suggest and it should be identical for both the ligand: every His deprotonation can give rise to the formation of a coordination bond and a ($2N_{Im}$, 2O) configuration can be hypothesized for both the species $[ZnLH_2]^+$ (in the case of L1) and $[ZnLH_3]^{2+}$ (in the case of L2), with a tetrahedral geometry. The oxygen atoms most likely belongs to water molecules in the

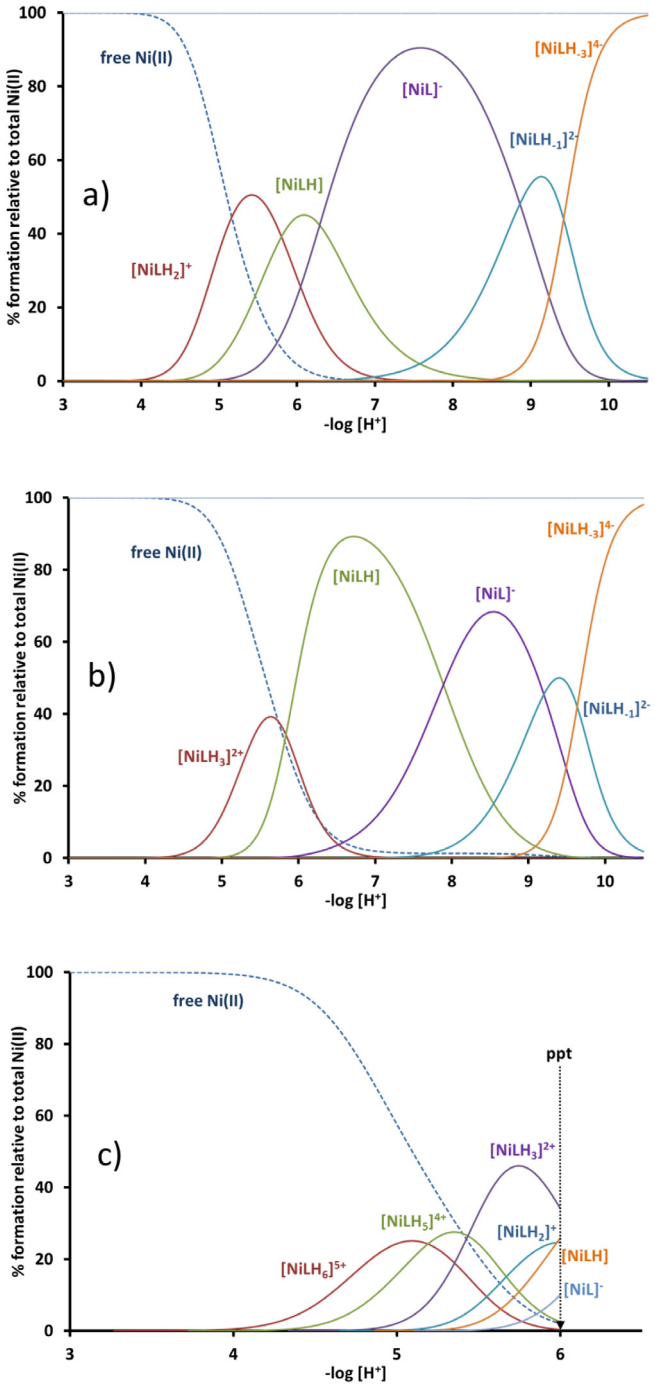

Fig. 1. Representative distribution diagrams for the complex-formation of the three peptides with Ni(II), at 298 K and I = 0.1 mol dm^{-3} (KCl). C°$_M$ = 5 · 10^{-4} mol dm^{-3}; M/L molar ratio = 1:1.2. (a) L1; (b) L2; (c) L3.

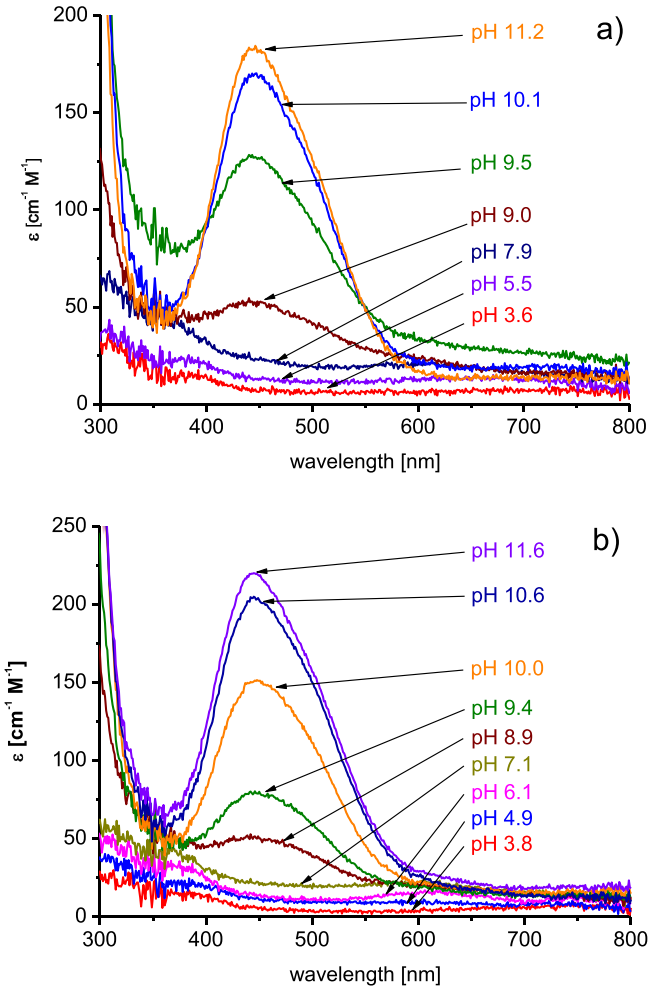

Fig. 2. Vis absorption spectra at variable pH for the binary solutions of the two short peptides with Ni(II), at 298 K and I = 0.1 mol dm^{-3} (KCl). C °$_M$ = 5 · 10^{-4} mol dm^{-3}; M/L molar ratio = 1:1.2. (a) L1; (b) L2.

first coordination sphere, although, in principle they could also come from the three carboxylate groups of the ligands. When pH is increased, the other His residues release their proton and can participate in complexation, leading to the very common (3N$_{Im}$, O) configuration, the same found in metalloproteases [1]. Once again, due to the abundance of donor atoms, many species with the same stoichiometry but different donor-atom sets can be present in solution at the same time, characterized by a fast exchange kinetics.

At the most alkaline pH values, the complexes [ZnLH$_{-1}$]$^{2-}$ and [ZnLH$_{-2}$]$^{3-}$ are formed in both the systems: although no spectroscopic confirmation is available for these species, the fitting of the corresponding potentiometric titration curves dramatically improves when they are considered in the speciation model. Different hypotheses on their structure can be put forward: a) deprotonation of amide nitrogens; b) deprotonation of pyrrole-like nitrogens of the coordinate His residues; c) deprotonation of coordinated water molecules. The first hypothesis is normally excluded in the literature and there is no new evidence here to support it; the pK_a values for the last two deprotonation steps look too small to suggest that the coordinate imidazole rings lose a further proton; deprotonation of coordinated water molecules is more common and likely. The stoichiometry of the species [ZnLH$_{-1}$]$^{2-}$ is compatible with the (3N$_{Im}$, O) configuration and a tetrahedral structure. On the other hand, in the case of the species [ZnLH$_{-2}$]$^{3-}$, since it is not likely that a OH$^-$ ligand substitutes an imidazole nitrogen of [ZnLH$_{-1}$]$^{2-}$, a change of geometry could be hypothesized, possibly leading to a penta-coordinated square-based pyramid or a trigonal bipyramid. These structures are less common but they have been found in proteins for both catalytic and structural zinc [48]. As a matter of fact, at pH > 9 further hydrolysis of the complex occurs.

The high similarity of the two speciation models would suggest that the presence of 4 or 5 His residues is mostly uninfluential for complex-formation behaviour. However, the competition plot shown in Fig. 6 shows that the higher number of histidines of L2 favours the first coordination of Zn(II) at acidic pH, while, in the

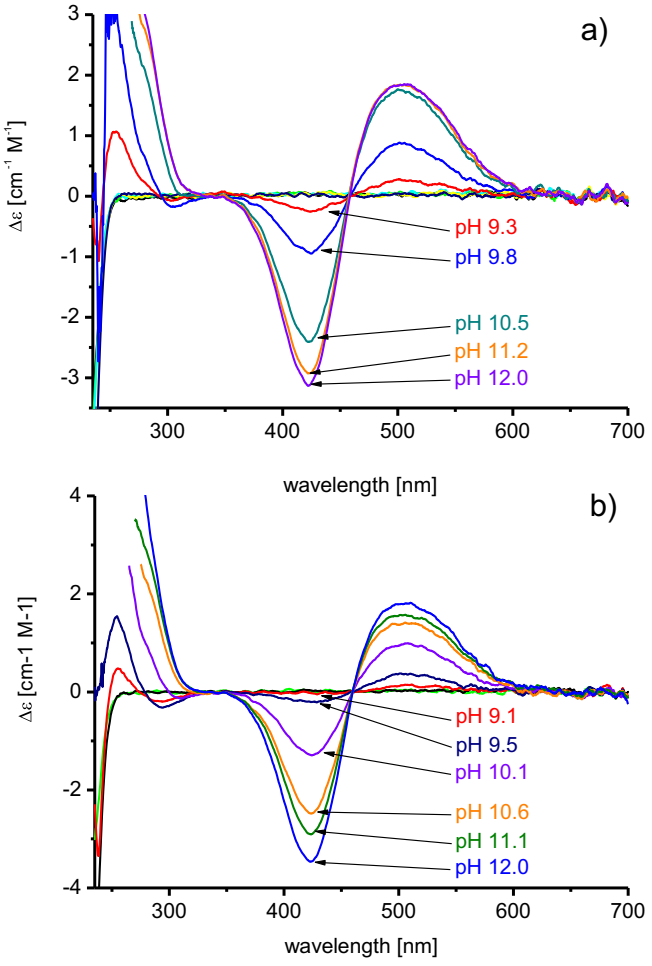

Fig. 3. Circular dichroism spectra at variable pH for the binary solutions of the two short peptides with Ni(II), at 298 K and $I = 0.1$ mol dm^{-3} (KCl). $C°_M = 5 \cdot 10^{-4}$ mol dm^{-3}; M/L molar ratio = 1:1.2. (a) L1; (b) L2.

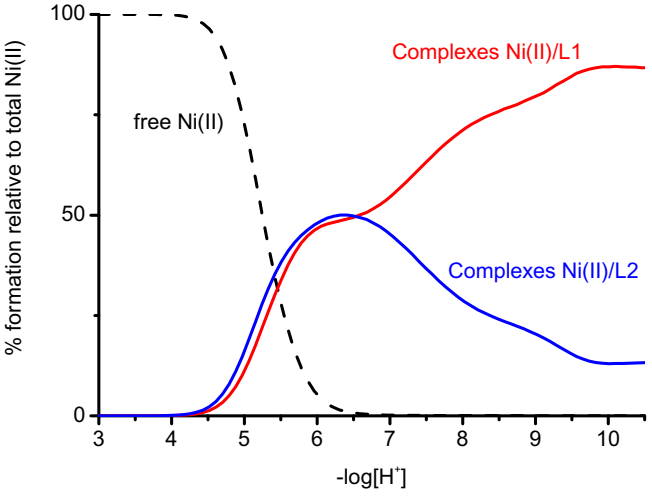

Fig. 4. Competition plot for a ternary solution containing equimolar amounts of Ni (II), L1 and L2.

alkaline pH range, L1 is preferred, in agreement with what already observed with nickel.

The distribution diagram of Fig. 5c shows that, in the case of L3, complex-formation starts at a pH = 4 and the first complex is the

Table 3
Cumulative complex-formation (β) and deprotonation (K_a) constants for binary Zn(II) complexes of the peptides L1, L2 and L3, at $T = 298$ K and $I = 0.1$ mol dm^{-3} (KCl). Standard deviations on the last figure in parentheses.

Ligand	Species	Log β	pK_a
L1	$[ZnLH_2]^{+}$	18.71 (9)	5.37
	[ZnLH]	13.34 (3)	6.48
	$[ZnL]^{-}$	6.86 (4)	8.15
	$[ZnLH_{-1}]^{2-}$	−1.29 (6)	9.17
	$[ZnLH_{-2}]^{3-}$	−10.46 (8)	–
L2	$[ZnLH_3]^{2+}$	25.0 (2)	5.15
	$[ZnLH_2]^{+}$	19.85 (5)	6.05
	[ZnLH]	13.80 (5)	7.23
	$[ZnL]^{-}$	6.57 (7)	8.65
	$[ZnLH_{-1}]^{2-}$	−2.08 (8)	9.2
	$[ZnLH_{-2}]^{3-}$	−11.3 (1)	–
L3	$[ZnLH_6]^{5+}$	45.07 (8)	–
	$[ZnLH_4]^{3+}$	35.02 (3)	–
	$[ZnLH_2]^{+}$	23.24 (4)	6.89
	[ZnLH]	16.35 (7)	6.85
	$[ZnL]^{-}$	9.50 (6)	8.45
	$[ZnLH_{-1}]^{2-}$	1.05 (9)	9.8
	$[ZnLH_{-2}]^{3-}$	−8.7 (1)	–

species $[ZnLH_6]^{5+}$, as already observed for Ni(II). Therefore, also in this case, three unprotonated imidazole side chains are available for complexation and it can be suggested that they really chelate the metal ion together with an additional oxygen donor. No precipitation was observed when pH was raised to the value of 10. Potentiometric data of Table 3 show that, increasing the pH, all the exchangeable protons are released and more nitrogen atoms, belonging to the remaining six imidazole side chains and the amino terminus, become available for complexation. It not possible to know, from the present data, if species are formed with a coordination geometry 4 N or higher, but this cannot be excluded. As a matter of fact, at pH 9 the two species $[ZnLH_{-1}]^{2-}$ and $[ZnLH_{-2}]^{3-}$ were detected: as already discussed above for L1 and L2, the deprotonation of water molecules bound to zinc can be suggested.

The influence of the number of His residues on the complex-formation ability towards the Zn(II) ion can be inferred from the competition plots of Figs. S10–S13 (Supplementary Information). As a general rule, in the acidic pH range, the efficacy (and perhaps the probability) of the first metal-binding interaction increases with the number of histidines contained in the peptide. Only in the case of the protected fragment of the Prion protein of Zebrafish (zp-PrP63-74) and L1, both containing 4 His residues, the "anchoring strength" at acidic pH is the same (Fig. S10a). In the alkaline pH range, where the coordination sphere of Zn(II) is saturated, the alternate Ala-His sequence of L1 is more effective than those of both zp-PrP63-74 [49] (Fig. S10a) and Ac-His-Sar-His-Sar-His-Sar-His-NH_2 [50] (Fig. S12), which contain the same number of histidines. Rather surprisingly, L1 and L2 peptides are also stronger ligands than zp-PrP63-80, which contains a series of -XXX-Gly-His-repetitions and a total of 6 His residues (Fig. S11).

Considering the peptide L3, it is clear that its binding strength is much higher than that of both L1 and L2 over the entire pH range (Fig. S13) and this is certainly due to the presence of 9 consecutive His residues. It would be interesting to clarify, with further experiments, the role played by the unprotected N-terminal amine of L3 on complex stability.

Finally, it is worth of note that L3 is a much stronger Zn(II) ligand also than the fragment of the zebrafish prion-protein zp-PrP63-87, containing seven (not consecutive) histidines [49], shown in the competition diagram of Fig. 7. Neglecting the difference in charge (due to the absence of carboxylate groups in the prion fragments), this observation supports again the conclusion that greater the number of His in a peptide and stronger is

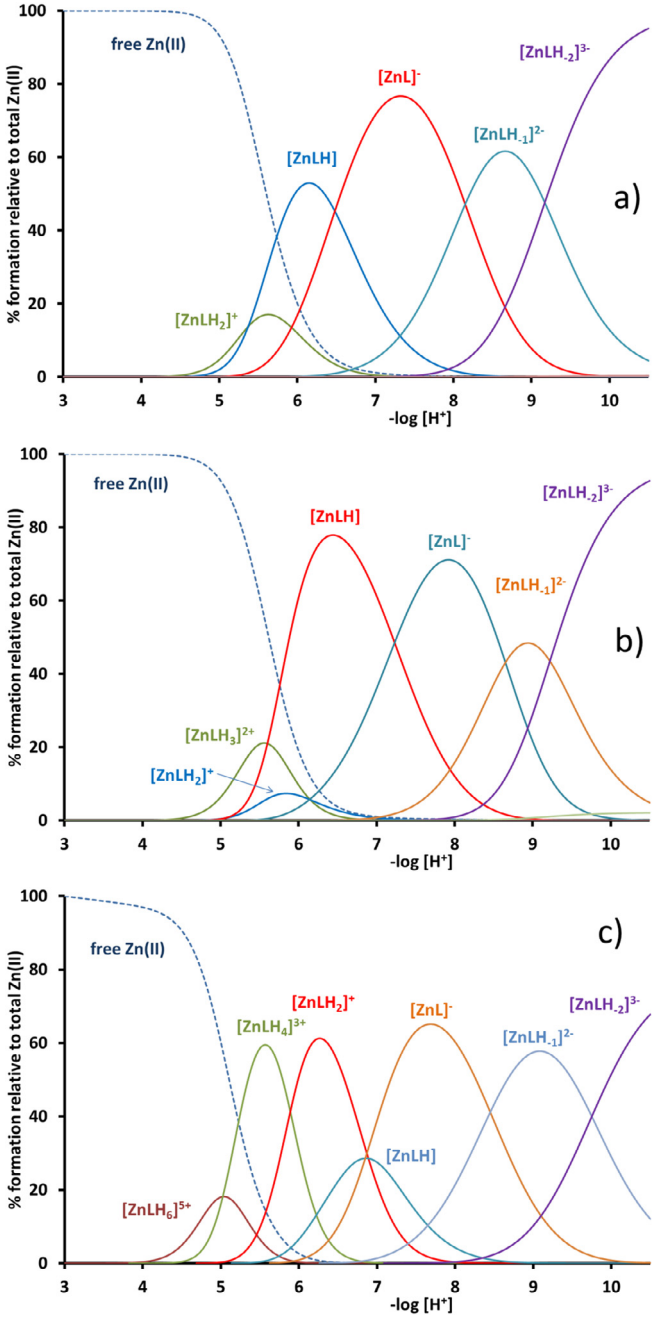

Fig. 5. Representative distribution diagrams for the complex-formation of the three peptides with Zn(II), at 298 K and $I = 0.1$ mol·dm^{-3} (KCl). $C°_M = 5{\cdot}10^{-4}$ mol·dm^{-3}; M/L molar ratio = 1:1.2. a) L1; b) L2; c) L3.

its coordination ability towards Zn(II). Obviously, it cannot be ruled out that also the presence of consecutive histidines plays a role in stabilizing the complex, favoring the coordination of more nitrogens and/or leading to the formation of a higher number of equivalent species with a similar geometry but a different set of donor atoms.

4. Conclusions

The present work confirmed that the peptides under investigation, containing several, consecutive or alternated with alanines, histidine residues, have the ability to tightly coordinate Ni(II) and

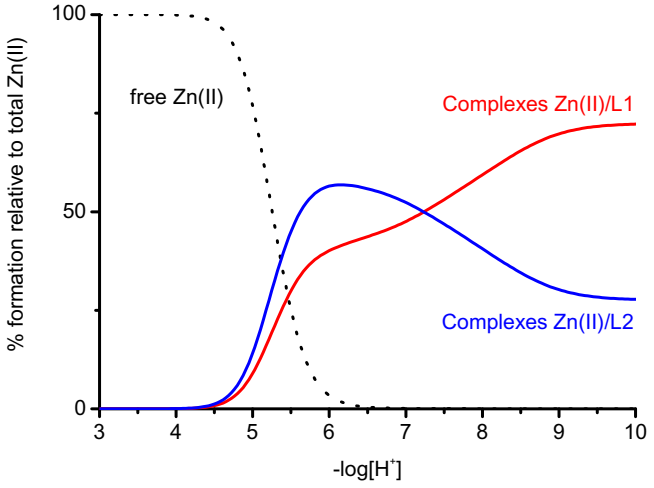

Fig. 6. Competition plot for a ternary solution containing equimolar amounts of Zn (II), L1 and L2.

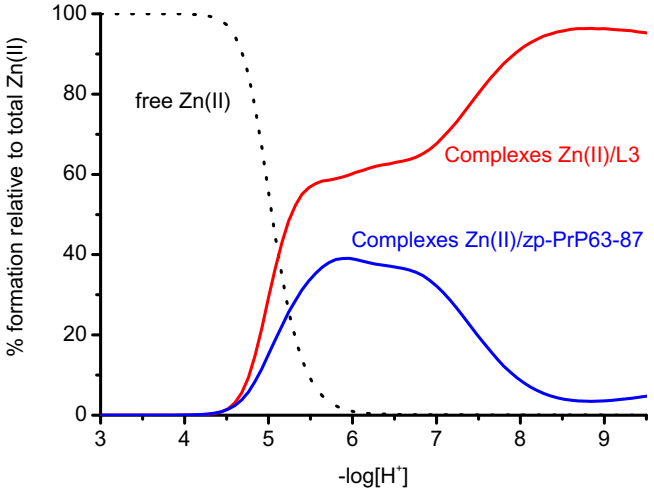

Fig. 7. Competition plot for a ternary solution containing equimolar amounts of Zn (II), L3 zp-PrP63-87 (Ac-PVHTGHMGHIGHTGHTGHTGSSGHG-NH_2) [49].

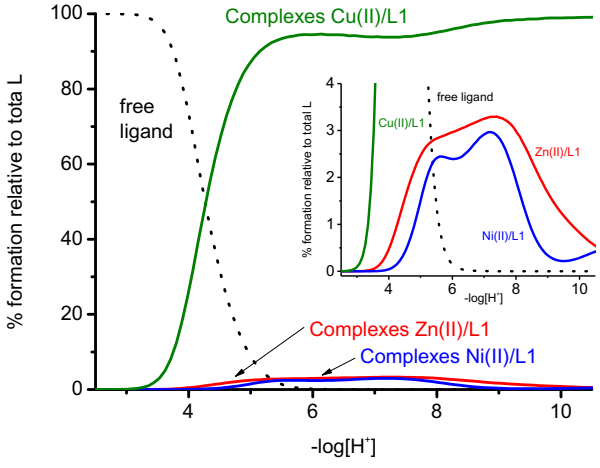

Fig. 8. Competition plot for a solution containing equimolar amounts of L1, Cu(II), Ni(II) and Zn(II).

Zn(II) ions, as previously reported for Cu(II) [28,32]. The competition plots reported in Figs. 8, S14 and S15 (Supplementary Information), show that complexes formed with copper are always by far the most stable throughout the explored pH range. Concerning the affinity for zinc and nickel, the insets reported in the figures show that the two metal ions have substantially the same binding ability towards the three peptides; Zn(II) is slightly preferred by the shorter ligands with alternate histidines while no significant difference was measured in the case of L3.

As for the role of histidines in the sequence of poly-His peptides in Ni(II) and Zn(II) complexation, the main conclusions of this work can be the following:

- the complex stability depends on both the number of histidines in the sequence and their relative position. Indeed, a high number of side imidazole rings can lead to many different combinations of nitrogen donors with the formation of several complexes with different structure but the same stoichiometry (entropic stabilizing factor). In addition, imidazoles build up a net of H-bonds which stabilize the complex. Moreover, the presence of helical-promoting Ala residues (which may restrain to some conformations) may be one of the reasons at the origin of the lower stability of the complexes of L1 and L2 compared to those of L3.
- In the case of Ni(II), the number of available imidazoles is the main stability-driving factor; moreover, at equal number, the peptides with consecutive histidines are favoured.
- In the case of zinc, the alternating His-Ala sequence leads to more stable complexes than other sequences of histidines; the alternating His-Ala sequence is also competitive with a XXX-XXX-His sequence (XXX is a generic amino acid), even when the number of histidines in the latter is higher.
- The very high affinity of the "snake peptide" L3 for Zn(II), the metal of the active site of metalloproteases, suggests that this is the key for the inactivation of the venom in the snake glands.

Finally, it would be interesting to confirm the structures of the complexes formed, the potential formation of polynuclear species and the individual role of histidines, using other analytical and/or computational techniques, such as NMR or DFT calculations. Another open point is the role of the amino-terminal group of L3, a good coordination site especially for Ni(II), which can promote the formation of macrochelates. All these topics will be the subject of further investigation.

Acknowledgements

The authors wish to thank the University of Ferrara (FAR 2015) for financial support and the CIRCMSB (Consorzio Interuniversitario di Ricerca in Chimica dei Metalli nei Sistemi Biologici, Bari, Italy).

Appendix A. Supplementary data

Supplementary data associated with this article can be found, in the online version, at http://dx.doi.org/10.1016/j.ica.2017.05.070.

References

[1] T.S. Kang, D. Georgieva, N. Genov, M.T. Murakami, M. Sinha, R.P. Kumar, P. Kaur, S. Kumar, S. Dey, S. Sharma, A. Vrielink, C. Betzel, S. Takeda, R.K. Arni, T.P. Singh, R.M. Kini, FEBS J. 278 (2011) 4544–4576.
[2] F.J. Vonk, K. Jackson, R. Doley, F. Madaras, P.J. Mirtschin, N. Vidal, BioEssays 33 (2011) 269–279.
[3] M.J. Bradshaw, A.J. Saviola, E. Fesler, S.P. Mackessy, Cytotechnology 68 (2016) 687–700.
[4] J.W. Fox, S.M.T. Serrano, Proteomics 8 (2008) 909–920.
[5] A. Onoda, T. Suzuki, H. Ishizuka, R. Sugiyama, S. Ariyasu, T. Yamamura, J. Pept. Sci. 15 (2009) 832–841.
[6] R. Marques-Porto, I. Lebrun, D.C. Pimenta, Comp. Biochem. Physiol. 147 (2008) 424–433.
[7] C. Ustun, I. Tegin, M.F. Geyik, J. Microbiol. Infect. Dis. 3 (2013) 71–74.
[8] A. Al-Asmari, N.A. Osman, A. Aziz, A.M. Aman, M.W. Khan, J. Biol. Sci. 1 (2013) 8–14.
[9] D.L. Menaldo, C.P. Bernardes, N.A. Santos-Filho, L.d.A. Moura, A.L. Fuly, E.C. Arantes, S.V. Sampaio, Biochimie 94 (2012) 2545–2558.
[10] A.F. Wahby, A.M. Abdel-Aty, E.M. El-Kady, Toxicon 59 (2012) 329–337.
[11] P. Favreau, O. Cheneval, L. Menin, S. Michalet, H. Gaertner, F. Principaud, R. Thai, A. Menez, P. Bulet, R. Stocklin, Rapid Commun. Mass Spectr. 21 (2007) 406–412.
[12] S.C. Wagstaff, P. Favreau, O. Cheneval, G.D. Laing, M.C. Wilkinson, R.L. Miller, R. Stoecklin, R.A. Harrison, Biochem. Biophys. Res. Commun. 365 (2008) 650–656.
[13] E. Salichs, A. Ledda, L. Mularoni, M.M. Alba, S. de la Luna, PLoS Genet. 5 (2009).
[14] D. Witkowska, R. Politano, M. Rowinska-Zyrek, R. Guerrini, M. Remelli, H. Kozlowski, Chem. Eur. J. 18 (2012) 11088–11099.
[15] D. Witkowska, M. Rowinska-Zyrek, G. Valensin, H. Kozlowski, Coord. Chem. Rev. 256 (2012) 133–148.
[16] D. Witkowska, D. Valensin, M. Rowinska-Zyrek, A. Karafova, W. Kamysz, H. Kozlowski, J. Inorg. Biochem. 107 (2012) 73–81.
[17] M. Rowinska-Zyrek, D. Witkowska, S. Potocki, M. Remelli, H. Kozlowski, New J. Chem. 37 (2013) 58–70.
[18] T. Cheng, W. Xia, P. Wang, F. Huang, J. Wang, H. Sun, Metallomics 5 (2013) 1423–1429.
[19] R. Vatansever, I.I. Ozyigit, E. Filiz, Turk. J. Biol. 40 (2016) 600–611.
[20] B.A. Eijkelkamp, V.G. Pederick, C.D. Plumptre, R.M. Harvey, C.E. Hughes, J.C. Paton, C.A. McDevitt, Infect. Immun. 84 (2016) 407–415.
[21] T.G. Nakashige, J.R. Stephan, L.S. Cunden, M.B. Brophy, A.J. Wommack, B.C. Keegan, J.M. Shearer, E.M. Nolan, J. Am. Chem. Soc. 138 (2016) 12243–12251.
[22] H. Du, S. Puri, A. McCall, H.L. Norris, T. Russo, M. Edgerton, Front. Cell Infect. Microbiol. 7 (2017).
[23] K. Terpe, Appl. Microbiol. Biotechnol. 60 (2003) 523–533.
[24] D.S. Waugh, Trends, Biotechnology 23 (2005) 316–320.
[25] H. Block, B. Maertens, A. Spriestersbach, N. Brinker, J. Kubicek, R. Fabis, J. Labahn, F. Schafer, in: R.R. Burgess, M.P. Deutscher (Eds.), Guide to Protein Purification, second ed., Elsevier Academic Press Inc, San Diego, 2009, pp. 439–473.
[26] S.W. Li, K.G. Yang, B.F. Zhao, X. Li, L.K. Liu, Y.B. Chen, L.H. Zhang, Y.K. Zhang, J. Mater. Chem. B 4 (2016) 1960–1967.
[27] J.X. Shi, J.M. Wong, J. Ma, T. Dickerson, C. Hall, D.A. Rock, T.J. Carlson, Bioanalysis 9 (2017) 251–264.
[28] F. Pontecchiani, E. Simonovsky, R. Wieczorek, N. Barbosa, M. Rowinska-Zyrek, S. Potocki, M. Remelli, Y. Miller, H. Kozlowski, Dalton Trans. 43 (2014) 16680–16689.
[29] J. Watly, E. Simonovsky, N. Barbosa, M. Spodzieja, R. Wieczorek, S. Rodziewicz-Motowidlo, Y. Miller, H. Kozlowski, Inorg. Chem. 54 (2015) 7692–7702.
[30] J. Watly, E. Simonovsky, R. Wieczorek, N. Barbosa, Y. Miller, H. Kozlowski, Inorg. Chem. 53 (2014) 6675–6683.
[31] E. Simonovsky, H. Kozlowski, Y. Miller, RSC Adv. 5 (2015) 104551–104555.
[32] D. Brasili, J. Watly, E. Simonovsky, R. Guerrini, N.A. Barbosa, R. Wieczorek, M. Remelli, H. Kozlowski, Y. Miller, Dalton Trans. 45 (2016) 5629–5639.
[33] M. Orfei, M.C. Alcaro, G. Marcon, M. Chelli, M. Ginanneschi, H. Kozlowski, J. Brasun, L. Messori, J. Inorg. Biochem. 97 (2003) 299–307.
[34] A. Janicka-Klos, P. Juszczyk, Z. Grzonka, H. Kozlowski, Polyhedron 27 (2008) 1511–1516.
[35] D. Valensin, L. Szyrwiel, F. Camponeschi, M. Rowinska-Zyrek, E. Molteni, E. Jankowska, A. Szymanska, E. Gaggelli, G. Valensin, H. Kozlowski, Inorg. Chem. 48 (2009) 9042.
[36] G. Zamariola, J. Watly, E. Gallerani, R. Gavioli, R. Guerrini, H. Kozlowski, M. Remelli, J. Inorg. Biochem. 163 (2016) 301–310.
[37] R.C. Dunbar, J. Martens, G. Berden, J. Oomens, Phys. Chem. Chem. Phys. 18 (2016) 26923–26932.
[38] W. Maret, J. Inorg. Biochem. 111 (2012) 110–116.
[39] H. Kozlowski, M. Luczkowski, M. Remelli, D. Valensin, Coord. Chem. Rev. 256 (2012) 2129–2141.
[40] H.M. Irving, M.G. Miles, L.D. Pettit, Anal. Chim. Acta 38 (1967) 475–488.
[41] P. Gans, B. O'Sullivan, Talanta 51 (2000) 33–37.
[42] P. Gans, A. Sabatini, A. Vacca, J. Chem. Soc., Dalton Trans. (1985) 1195–1200.
[43] G. Gran, Acta Chem. Scand. 4 (1950) 559–577.
[44] P. Gans, A. Sabatini, A. Vacca, Talanta 43 (1996) 1739–1753.
[45] L. Alderighi, P. Gans, A. Ienco, D. Peters, A. Sabatini, A. Vacca, Coord. Chem. Rev. 184 (1999) 311–318.
[46] C.F. Baes, R.E. Mesmer, The Hydrolysis of Cations, John Wiley & Sons Ltd, New York, 1976.
[47] H. Kozlowski, A. Lebkiri, C.O. Onindo, L.D. Pettit, J.F. Galey, Polyhedron 14 (1995) 211–218.
[48] I.L. Alberts, K. Nadassy, S.J. Wodak, Protein Sci. 7 (1998) 1700–1716.
[49] L. Szyrwiel, E. Jankowska, A. Janicka-Klos, Z. Szewczuk, D. Valensin, H. Kozlowski, Dalton Trans. (2008) 6117–6120.
[50] C. Kallay, K. Varnagy, G. Malandrinos, N. Hadjiliadis, D. Sanna, I. Sovago, Inorg. Chim. Acta 362 (2009) 935–945.